JOURNAL OF CATALYSIS **164,** 268–275 (1996)
ARTICLE NO. 0383

The Characterisation of Distinct Adsorption Sites for Hydrogen on Copper in Copper/Alumina Catalysts by *in Situ* ^{1}H NMR Spectroscopy

J. B. C. Cobb, A. Bennett, G. C. Chinchen,* L. Davies,* B. T. Heaton, and J. A. Iggo[1]

*Department of Chemistry, University of Liverpool, P.O. Box 147, Liverpool L69 3BX, United Kingdom; and *ICI Katalco, R&T Group, P.O. Box 1, Billingham, Cleveland TS23 1LB, United Kingdom*

Received February 13, 1995; revised June 7, 1996; accepted August 21, 1996

Two distinct hydrogen adsorption sites on the copper component of a copper/alumina catalyst have been identified by monitoring the adsorption of hydrogen using *in situ* ^{1}H NMR spectroscopy. The NMR spectra reveal that one type of adsorption site is associated with relatively large, smooth copper particles whilst the other comprises a family of adsorption sites probably associated with faceting and defect sites on smaller copper particles. Exchange between the two types of adsorption site is surprisingly slow, with an upper limit for exchange of 2500 s^{-1}, whilst exchange amongst the family of sites associated with the smaller particles, although still slow, is faster, of the order of milliseconds. Spillover exchange of hydrogen between the copper surface and the support is shown to be negligible on the timescale of the spin–lattice relaxation (tens of milliseconds). TPR, XRD, and optical and electron microscopy investigations of the catalyst precursors did not predict the differences between the catalyst samples.

INTRODUCTION

The characterisation of catalysts and the determination of sites for adsorption is an important part of catalyst science. NMR spectroscopy has recently been identified as a promising addition to the array of techniques available. NMR studies have been reported that describe the adsorption of hydrogen on and spillover of hydrogen between the various catalyst components on copper (1, 2) and mixed copper–ruthenium (3) catalysts on a variety of oxide supports. For example, Dennison *et al.* (1) observed hydrogen atoms chemisorbed on the copper as well as hydrogen on both of the oxide phases and hydroxyl groups on zinc oxide in a study of a $Cu/ZnO/Al_2O_3$ catalyst. Wu *et al.* (3) studied the adsorption of hydrogen on 5% Cu/SiO_2 and $Ru–Cu/SiO_2$ impregnated catalysts and found hydrogen adsorption to occur on both copper and ruthenium. The copper was proposed to be present in two forms: an overlayer on the ruthenium and, in those catalysts with a bulk copper composition greater than 45%, as large Cu islands on the Ru–Cu bimetallic particles or separate copper particles. The basis for these conclusions was the existence or not of a discrete resonance for hydrogen on copper in the ^{1}H NMR spectrum and the variation in the Knight shift of the hydrogen on ruthenium with copper content. Two types of hydrogen on copper were claimed to be present: (i) molecular and (ii) atomic.

In this paper we report a study of several copper/alumina catalysts of nominally similar composition for which the first indication of differences in the copper morphology between the samples was provided by an *in situ* NMR investigation of hydrogen adsorption.

METHODS

Materials

Catalysts are referred to by their components and laboratory code. For example, the copper oxide/alumina catalyst, laboratory code U6649, is written as CuO/Al_2O_3 (U6649). Catalyst samples which have been activated in H_2 are indicated by writing the copper component as copper metal, e.g., Cu/Al_2O_3 (U6649).

Four samples were prepared by coprecipitation of the nitrates (HNO_3, $Al(NO_3)_3 \cdot 9H_2O$, Na_2CO_3, BDH, GPR grade; $Cu(NO_3)_2 \cdot 3H_2O$, BDH "Analar" grade). All four samples were precipitated to pH 7.2 ± 0.2 at 40°C, the precipitates washed to constant conductivity to remove sodium and subjected to the same purification, drying and calcination regimes, viz. 12 h at 120°C followed by 6 h at 350°C. A difference in source of the aluminium nitrate divides the samples into two groups U6649 and U6779 from BDH, U6778 and U6776 from ICI Katalco. The CuO : alumina ratio in U6778 is 1 : 1.1 whereas in the other three samples this ratio is 1 : 1.3. The CuO/Al_2O_3 powders were examined by optical microscopy (×400) and judged to be homogeneous.

Typically, catalysts were activated in a hydrogen gas stream, ca. 10 lh^{-1} for 12 h at 488 K.

[1] To whom correspondence should be addressed. Fax: 0151 794 3588. E-mail: iggo@liv.ac.uk.

0021-9517/96 $18.00

Instrumentation

A Bruker WM 200 WB spectrometer operating at 4.7 T was used for this work. This spectrometer was intended for solution work and is equipped with a slow digitiser. Severe baseline roll is seen in all the spectra. This is due to electrical ringing from the decaying excitation pulse. The *in situ* NMR probes used in this work have been described elsewhere (2, 4, 5). All ^{1}H NMR spectra are referenced to hydrogen gas at 0.0 ppm at 298 K, 1.0 bar. Shifts are accurate to $\pm$0.5 ppm; relative shifts for a given experiment are accurate to $\pm$0.1 ppm.

Slight shifts, ca. 1 ppm, were noted between samples and are thought to reflect the degree of reduction of the copper surface; supported copper is notoriously difficult to reduce fully.

T_1 relaxation times were determined by three methods: inversion-recovery, saturation recovery using a saturating comb pulse train, and selective saturation recovery. Prior to each T_1 determination, the 180° pulse was measured on a liquid sample and/or the catalyst and found to be in the range 32 to 38 μs.

The baseline roll, low intensity, and breadth of the resonances made it difficult accurately to ascertain the intensity of the resonance under investigation and accounts for the majority of the error in the measurements. Various data manipulations, e.g., left shifting, were tried to "enhance" the spectra. These were found not to alter the T_1 values significantly but did result in loss of information about the broad resonances. "Raw" spectra were used in the T_1 determinations reported here and are presented in the figures. T_1 relaxation times were determined by least squares fitting of the measured *intensity* of the NMR resonances to

$$M_t = M_0 \left[1 - A\, e^{\frac{-t}{T_1}}\right], \qquad [1]$$

where M_t is the z magnetisation at time t after the π pulse/application of the saturating irradiation and T_1 is the relaxation time constant. A is nominally 2 in the inversion recovery experiment and 1 in the saturation recovery experiments. M_0 is nominally the Boltzman equilibrium value of the magnetisation. M_0, A, and T_1 were treated as variables to be fit in the inversion recovery data to allow for mis-setting of the pulse lengths and incomplete relaxation between FIDs. The saturation recovery methodologies should be relatively insensitive to these errors and A was set to 1 in the analysis of the data from these experiments. The T_1 relaxation times in the inversion recovery experiments have also been approximated from the null point of the resonance. All values reported are the average of at least two determinations and are considered accurate to ca. $\pm$5 ms. The inversion-recovery method is likely to underestimate the true spin–lattice relaxation time due to errors in setting the pulse lengths. This problem was particularly acute for experiments performed in the metal pressure vessel (2).

The large sweep width used in these *in situ* NMR experiments coupled with the long pulse lengths achievable with our instrument results in uneven excitation across the spectrum. It was therefore not possible to measure the spin–lattice relaxation of the chemically shifted resonances and the Knight-shifted resonances simultaneously using the inversion-recovery sequence. The T_1 relaxation of the Knight-shifted and the chemically shifted resonances were therefore determined by adjusting the O1 value to place the resonance under investigation in the centre of the spectrum. This allows approximately uniform, selective, excitation of this resonance.

Temperature-programmed reductions of U6649 and U6776 were measured on Micromeritics 2900 equipment using a thermal conductivity detector. The heating rate was 20°C/min and the reduction gas was 5% hydrogen in nitrogen.

XRD spectra were recorded on a Philips 1730 diffractometer using copper radiation. This gave a rising background. The spectra were also recorded on a D4 Siemens D5000 instrument, using cobalt radiation to eliminate the fluoresence effect and allow inspection of the diffraction scan background. TEM were recorded on a JEOL 1200 EX Instrument.

RESULTS

CuO/Al_2O_3 (U6649)

After activation of the sample and evacuation of the reactor vessel, the ^{1}H NMR spectrum, recorded at 298 K, consisted of a weak broad resonance at $-$3.7 ppm superimposed on the baseline roll. The reactor vessel was then pressurised to 10 mbar with H_2 when two very low intensity resonances were observed in the Knight shifted region of the ^{1}H NMR spectrum at approximately 90 ppm and 83 ppm (Fig. 1a). The downfield resonance is sharper than the upfield resonance. These resonances increase in intensity on sequentially increasing the pressure to 20, 50, 100 mbar and shift upfield. There was a slight increase in the intensity of the resonance in the chemically shifted region until at 100 mbar a broader resonance emerged. Above 100 mbar the broader resonance in the chemically shifted region increased in intensity to dominate the region. The intensities of the Knight-shifted resonances were essentially unchanged by further increases in pressure and were still visible at 43 bar (Table 1).

CuO/Al_2O_3 (U6776)

After activation of the sample and evacuation of the reactor vessel, hydrogen gas was admitted. Resonances were observed at 0.0 ppm and 85.4 ppm in the ^{1}H NMR spectrum (Fig. 1b).

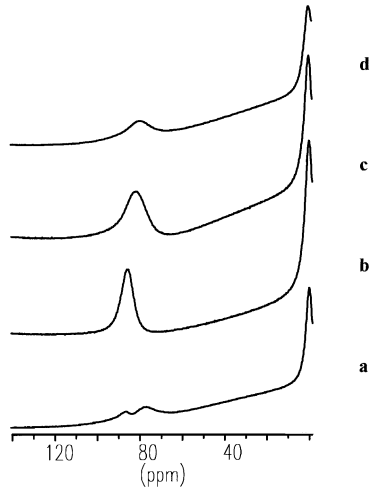

FIG. 1. ^{1}H *in situ* NMR spectrum of (a) Cu/Al_2O_3 (U6649), (b) Cu/Al_2O_3 (U6776), (c) Cu/Al_2O_3 (U6778), and (d) Cu/Al_2O_3 (U6779) in the presence of 1 atm hydrogen gas.

CuO/Al_2O_3 (U6778)

After activation of the sample and evacuation of the reactor vessel the ^{1}H NMR spectrum showed a very weak Knight-shifted resonance at approximately 83 ppm. A weak resonance was also observed at approximately −4 ppm. On admission of hydrogen to the vessel there was an increase in the intensity of the Knight-shifted resonance. When the H_2 pressure was raised to 0.10 bar there was a large increase in the intensity of the Knight-shifted resonance which shifted downfield to 87.6 ppm (Fig. 1c).

CuO/Al_2O_3 (U6779)

After activation of the sample and evacuation of the reactor vessel the vessel was pressurised with H_2. A Knight-shifted resonance at 82.5 ppm was observed in the ^{1}H NMR spectrum. On increasing the pressure there was little change in the intensity of the Knight-shifted resonance which shifted further upfield to 80.6 ppm at 2.00 bar (Fig. 1d).

TABLE 1

Pressure Dependence of the Knight Shift of Hydrogen Adsorbed on the Cu/Alumina Catalyst, CuO/Al_2O_3 (U6649)

Pressure (mbar)	Knight shift (δ/ppm)	Chem. shift (δ/ppm)	$W_{1/2}$/Hz Knight shift
0	—	−3.7	
10	90.0, 83.0	−3.7	
20	91.4, 84.1	−3.7	
50	89.0, 83.2	−3.4	
100	88.1, 82.9	−2.7	
200	87.5, 82.7	0.4	
300	87.0, 82.6	0	
500	86.5, 82.4	0.1	
3000[a]	84.9, 73.9	0.0	820, 2500
43000[a]	82.2, 71.1	−0.5	

[a] Second sample, "new" probe (5).

TABLE 2

Spin Lattice Relaxation Data for Hydrogen Adsorbed on the Cu/Alumina Catalyst, Cu/Al_2O_3 (U6649)

Method	T_1/ms $\delta \approx 87$ ppm	$\delta \approx 82$ ppm	$\delta \approx 5$ ppm	$\delta \approx 0$ ppm
Inversion recovery (least squares fit)	67 ± 2	42 ± 2	Not recorded	Not recorded
Inversion recovery (null point) sample 2	58 ± 6	43 ± 6	4 ± 2	2 ± 2
Inversion recovery (null point) sample 1	36 ± 4	36 ± 4	2 ± 2	0.5 ± 0.5
Saturation recovery (selective saturation)	65 ± 2	Not recorded	Not recorded	Not recorded
Saturation recovery (comb saturation)	65 ± 2	Not recorded	Not recorded	Not recorded

Exchange between Copper Adsorption Sites and Copper Particles in Cu/Al_2O_3 (U6649)

Spin–lattice relaxation times of hydrogen adsorbed on Cu/Al_2O_3 (U6649). Two samples of Cu/Al_2O_3 (U6649) were activated in flowing H_2 for 12 h at 488 K. After activation, the vessel was evacuated at 453 K, cooled to 298 K and then pressurised with 1.00 bar H_2 (sample 1), or allowed to cool to 295 K, evacuated and then pressurised to 0.360 bar (sample 2). Spin–lattice relaxation times are given in Table 2. Figures 2 and 3 show representative partially relaxed spectra for sample 2. A comparison of the relaxation data from these experiments gives information on the

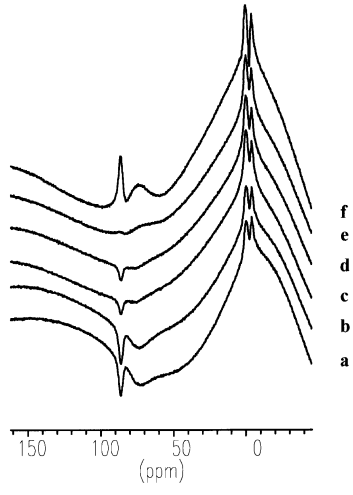

FIG. 2. Partially relaxed ^{1}H *in situ* NMR spectra of hydrogen adsorbed on Cu/Al_2O_3 (U6649), inversion recovery sequence centred at 75 ppm; t = (a) 1 μs, (b) 1 ms, (c) 3 ms, (d) 20 ms, (e) 60 ms, and (f) 1000 ms.

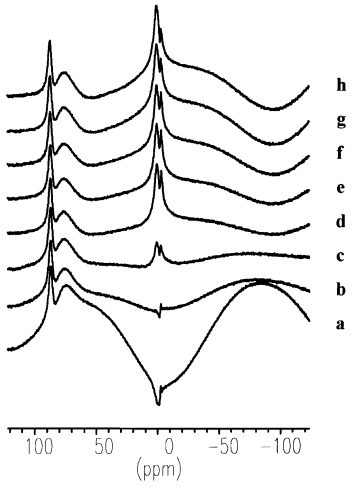

FIG. 3. Partially relaxed ^{1}H *in situ* NMR spectra of hydrogen adsorbed on Cu/Al_2O_3 (U6649), inversion recovery sequence centred at 0 ppm; $t =$ (a) 1 μs, (b) 1 ms, (c) 3 ms, (d) 20 ms, (e) 60 ms, (f) 200 ms, (g) 500 ms, and (h) 1000 ms.

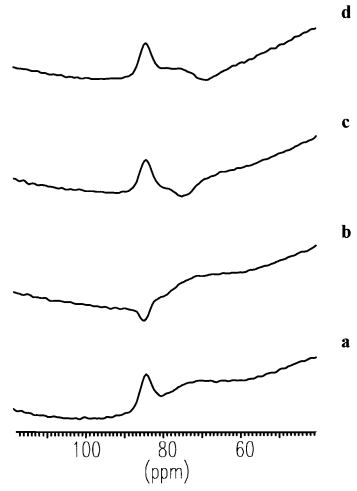

FIG. 4. ^{1}H *in situ* NMR spectrum of Cu/Al_2O_3 (U6649) in the presence of hydrogen gas showing the effect of inhomogeneous broadening. Conditions: 3 ms acquisition, 1 ms pre-irradiation (a) 6 kHz off resonance, (b) at centre of downfield Knight-shifted peak, (c) at high-frequency edge of upfield Knight-shifted peak, and (d) at low-frequency edge of upfield Knight-shifted peak.

possible existence of exchange processes occurring on the timescale of the relaxation or faster. The saturating comb experiment evenly excites the entire spectrum whereas the selective saturation and inversion recovery (*vide supra*) methods excite selected regions of the spectrum. If exchange is occurring on the timescale of the relaxation or faster, spin–lattice relaxation may occur via exchange with the pool of hydrogen nuclei not excited by the 180° pulse/selective irradiation, i.e., hydrogen in the gas phase and hydrogen adsorbed on the support. This pathway is not present in the saturating comb experiment. Thus, if exchange is occurring on the timescale of the relaxation or faster, the saturating comb measurement will give a longer apparent value for the spin–lattice relaxation time than the other two experiments (1). The relaxation rates of the two Knight-shifted peaks differ, the broad upfield peak relaxing slightly faster, $T_1 = 42$ ms, than the downfield resonance, $T_1 = 66$ ms. The values obtained are invariant with the methodology used in the measurement, indicating that there is no significant exchange of hydrogen between the copper sites and the support or gas phase on the timescale of the relaxation. The relaxation of the hydrogen gas in the vessel and of the oxide associated hydrogens is much faster than that of the copper associated hydrogen; in these cases the T_1 is of the order of 1–2 and 4 ms, respectively. The relaxation times for sample 1 were determined using the metal pressure vessel and are generally shorter as a consequence of the greater difficulty in accurately setting the 180° pulse in this cell.

Saturation transfer. The resonances due to hydrogen on copper are inhomogeneously broadened; i.e., the linewidth is due, in part, to the existence of a distribution of adsorption sites within each resonance envelope, each adsorption site having a slightly different Knight shift. Irradiation at a specific frequency within the resonance envelope will only affect those hydrogens that resonate at that frequency; there will be no transfer of saturation to hydrogens associated with other copper adsorption sites unless exchange between the sites is occurring. This will be true both for exchange between two copper particle "types" and for exchange between adsorption sites on any copper particle. Two irradiation regimes were used. In the first, relatively high power irradiation was applied at a selected frequency within each resonance envelope or 6 kHz off resonance for 1 ms. An acquisition time of ca. 3 ms was used in order to minimise the effects of relaxation and exchange. The spectra in Fig. 4

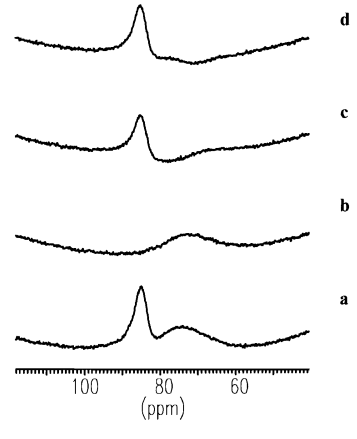

FIG. 5. ^{1}H *in situ* NMR spectrum of Cu/Al_2O_3 (U6649) in the presence of hydrogen gas showing the effect of inhomogeneous broadening. Conditions: 12 ms acquisition, 100 ms pre-irradiation (a) 6 kHz off resonance, (b) at centre of downfield Knight-shifted peak, (c) at high-frequency edge of upfield Knight-shifted peak, and (d) at low-frequency edge of upfield Knight-shifted peak.

show the characteristic "burn out" in the resonance envelope expected for an inhomogeneously broadened NMR line. The second regime used a relatively low power irradiation for 100 ms and an acquisition time of ca. 12 ms to allow transfer of the saturation via site exchange. This resulted in saturation of the entire envelope of the resonance within which the radiation was applied but little or no saturation of the other envelope (Fig. 5). Thus exchange between adsorption sites in a given resonance envelope is relatively fast but exchange of hydrogen between resonance envelopes is slow. These results are most easily explained if the two resonance envelopes are attributed to hydrogen adsorbed on separate copper particles of different morphologies.

Similar experiments to study exchange between the gaseous hydrogen and/or the oxide associated hydrogen and the hydrogen on copper gave no evidence for exchange on the timescale of these experiments.

TPR. The TPR profiles of U6776 and U6649 catalysts are shown in Fig. 6. The profiles are broadly similar. That of U6776 shows an intense peak at 300°C assigned to the reduction of copper oxide to copper metal and a very weak peak at 455°C, (Fig. 6A). The profile of the U6649 catalyst shows an intense peak at 278°C, a peak at 345°C, and a very weak peak at approximately 470°C. The peaks at 278 and 345°C are assigned to the reduction of two types of copper oxide species. A second TPR profile (reducing gas 5% H_2 in He, 60 ml/min) of this sample (30 mg) confirms the presence of two copper oxide reduction peaks (Fig. 6B). It is possible that the two types of copper oxide associated with these reduction peaks are the precursors to the two types of copper particles associated with the two Knight-shifted resonances.

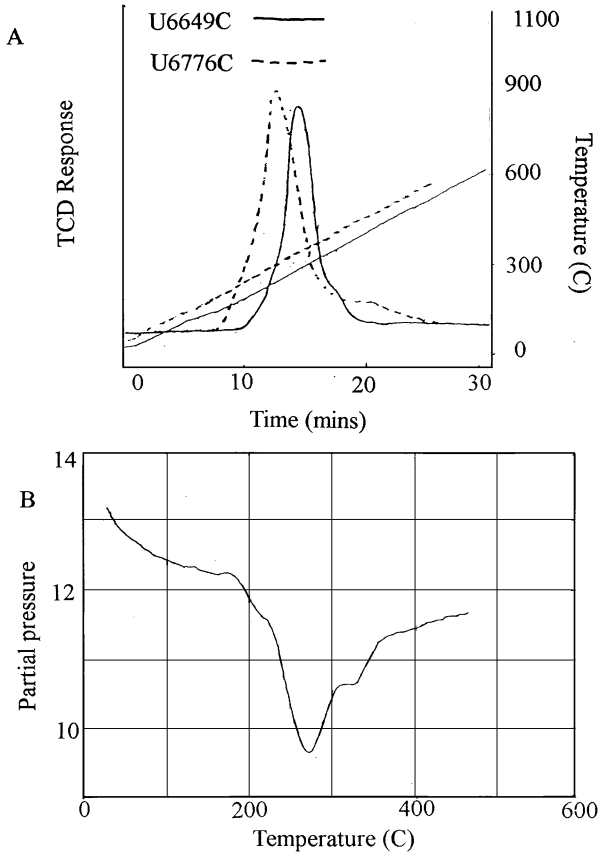

FIG. 6. TPR profiles of (A) CuO/Al_2O_3 (U6649) (—) and CuO/Al_2O_3 (U6776) (- - -); (B) CuO/Al_2O_3 (U6649); for conditions see text.

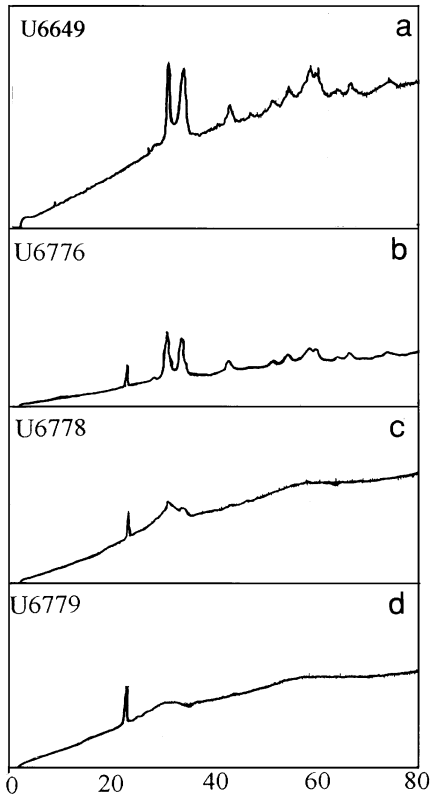

FIG. 7. XRD profiles of (a) CuO/Al_2O_3 (U6649), (b) CuO/Al_2O_3 (U6776), (c) CuO/Al_2O_3 (U6778), and (d) CuO/Al_2O_3 (U6779).

XRD. The XRD spectra of the four catalysts are shown in Fig. 7. Samples CuO/Al_2O_3 (U6649) and CuO/Al_2O_3 (U6776) contain large crystallites of copper oxide in the form of tenorite whereas CuO/Al_2O_3 (U6778) and CuO/Al_2O_3 (U6779) contain only amorphous copper oxide as evidenced by the broad overlapped peaks in the region expected for tenorite. Although no alumina phase could be identified from the diffraction data there are regions of intensity in the scans which indicate the presence of an amorphous phase, probably a transition alumina. This effect was most evident in CuO/Al_2O_3 (U6778) and CuO/Al_2O_3 (U6779).

TEM. Transmission electron micrographs of CuO/Al_2O_3 (U6649) catalyst have been obtained (Fig. 8). Small, darker spots can be seen against lighter patches which have

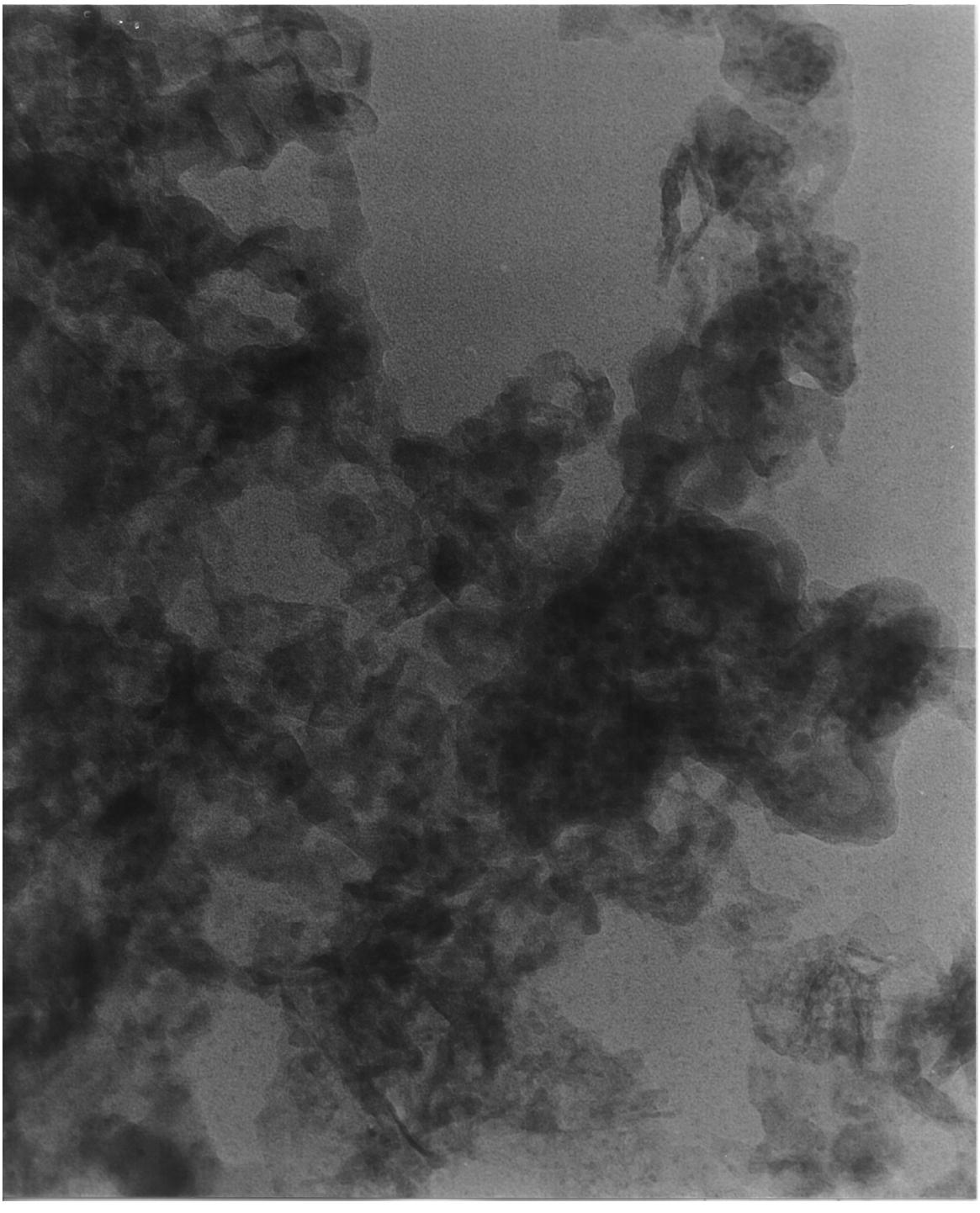

FIG. 8. TEM image of CuO/Al_2O_3 (U6649) (magnification × 750,000).

been identified as CuO particles on the amorphous Al_2O_3 support. The CuO particles are between 10 and 60 Å in diameter, with an average diameter between 15 and 20 Å. There is clearly a considerable difference in the diameters of the CuO particles; however, it is not clear whether there is a bimodal CuO particle distribution.

DISCUSSION

A number of studies have attempted to measure the copper particle size on typical catalysts. The particle sizes proposed have varied considerably. XRD studies have typically indicated copper particle sizes of the order of hundreds

of angstroms (6–8). Klier and co-workers report a transition from small particles (<20 Å) to larger particles (>200 Å) as the copper content exceeds 30% (9).

Frost (10) studied copper/thoria catalysts with XRD and *in situ* EXAFS and found that there were two forms of copper metal particle, namely large (>100 Å) and very small (7–15 Å) particles. The small copper particles made up 95% of the total copper.

Tohji *et al.* (11) studied a coprecipitated Cu/ZnO catalyst with a 3 : 7 Cu : Zn ratio with *in situ* EXAFS and concluded that the morphology of the copper particles varied with temperature. Below 400 K the copper particles existed as a quasi-two-dimensional epitaxial layer over the zinc oxide. There was evidence in the EXAFS data for Cu–O bonds at the interfacial region. Above 400 K the copper was in the form of small metal particles. The diameter of these particles was 20–30 Å.

In summary it appears that two types of copper particle exist on coprecipitated catalysts. The copper particles of Cu/ZnO and Cu/Al_2O_3 catalysts with low copper contents exist as small particles about 5–20 Å in diameter. On higher copper content (>30%) Cu/ZnO catalysts both large copper crystallites (around 200–300 Å in diameter) and small copper particles are present. Small particles will have a high population of defect sites and a larger proportion of higher index plane faces than larger particles. Wu *et al.* (3) and others have proposed that hydrogen gas dissociatively adsorbs on high index copper planes and defect sites. Therefore, it would be expected that hydrogen would more readily adsorb on the small (10–40 Å) copper particles rather than the larger (>100 Å) copper particles.

In this study of a series of Cu/Al_2O_3 catalysts, *in situ* NMR clearly reveals the existence of two distinct copper sites for the adsorption of hydrogen on copper in Cu/Al_2O_3 (U6649) whereas only one site is seen in all the other samples. XRD reveals that in two of the samples, CuO/Al_2O_3 (U6649) and CuO/Al_2O_3 (U6776), there are large crystallites of tenorite in contrast to the other two samples in which the copper oxide is largely amorphous. The crystallinity of the CuO/Al_2O_3 precursor appears to show some correlation with the size of the Knight shift and the breadth of the NMR resonance for hydrogen on copper for the samples U6776, U6778, and U6779. Thus the most shifted, sharpest line is found for the most crystalline sample, U6776, whilst the broadest, least shifted is the highly amorphous U6779. U6649 shows resonances that might then be attributed to hydrogen adsorbing on copper both from crystalline and from amorphous CuO/Al_2O_3 precursors. TEM (Fig. 8) revealed that the CuO particles are between 10 and 60 Å in diameter in U6649 with an average diameter between 15 and 20 Å and that there is clearly a considerable difference in the diameters of the CuO particles, although it is not clear whether both amorphous and crystalline CuO/Al_2O_3 are present.

The Knight shift of hydrogen adsorbed on a metal surface is determined by the contact interaction between the metal conduction electrons and the hydrogen nuclear spin. The Knight shift is thus characteristic for a particular metal and will be affected both by physical attributes of the metal particle such as size and surface structure and by the presence of coadsorbates. The observation of two Knight shifted resonances for hydrogen on copper on sample Cu/Al_2O_3 (U6649) is therefore indicative of two different copper adsorption sites for hydrogen in this catalyst. Both Knight shifts are in the region expected for adsorption of hydrogen on a relatively clean copper surface (1–3). The differing linewidth of the two sites has several possible explanations:

(i) Paramagnetic impurities may be clustered around one adsorption site.

(ii) More restricted motion of the hydrogen in the upfield site giving less effective averaging to zero of dipole–dipole, chemical shift anisotropy, and other line broadening interactions.

The double irradiation experiments militate against both these explanations; the "hole" burnt into the resonance envelopes of the two sites is of similar width implying that the "extra" linewidth of the upfield resonance is not due to a homogeneous broadening effect.

(iii) A family of adsorption sites, each giving a slightly different Knight shift, is associated with each resonance envelope.

This last explanation will result in inhomogeneous broadening of the resonance and is consistent with the double resonance experiments; only those nuclei that are on resonance will be affected by the saturating radiation and a hole will be burnt in the absorption envelope. The observation that the whole resonance line is saturated if low-power irradiation is applied over a longer time indicates that exchange is occurring between the sites within each family albeit at a surprising low rate; irradiation for at least 20 ms is needed to allow the saturation to "exchange out" over all sites in the resonance envelope. Exchange between the two families is slower still; transfer of saturation is not complete even after 500 ms irradiation although relaxation occurring during the migration of the hydrogen across the support may reduce the apparent transfer due to the short relaxation time for hydrogens on the oxide phase.

If the difference in the linewidths is due to the spread of Knight shifts in each family of adsorption sites it is likely that the broader resonance reflects a rougher surface, indicating smaller or/and less crystalline particles. The broader resonance also has a smaller Knight shift, implying a lower conduction electron density, again not inconsistent with smaller particles. The linewidth of the more Knight-shifted, narrower resonance is similar to the width of the hole burnt in the hydrogen on copper resonance on a copper/zinc oxide/alumina particle (12), suggesting that the linewidth is

due principally to homogeneous broadening and not to a spread of Knight shifts. This suggests that this resonance is associated with a smooth surface, indicating a more crystalline and/or larger copper particle. Thus reduced U6649 appears to contain two types of copper particle, namely small, rough particles and smooth, large particles. The XRD results suggest that the crystallinity of the precursor may be a factor in determining the type of copper particle in the reduced catalyst. An alternative explanation of the presence of two adsorption sites for hydrogen in U6649 is that distinct adsorption sites exist on a single copper particle; however, it is difficult to reconcile this view with both slow exchange between sites as revealed by the "hole burning" experiments and the highly mobile nature of the hydrogen on the copper surface as revealed by the sharp NMR resonances.

The observation of only a single Knight-shifted resonance for hydrogen adsorbed on copper for all the other catalysts in this and other studies (1–3, 12) indicates that the bimodal copper particle distribution in Cu/Al_2O_3 (U6649) is not characteristic of copper/alumina catalysts.

The observation of different spin–lattice relaxation times for the two resonances is further evidence for slow exchange of hydrogen between the two families of sites since exchange must be slow on the timescale of the relaxation, viz. tens of milliseconds, in order not to average the relaxation times between families. Thus it would seem that migration of hydrogen between the copper particles is slow. A limit can be put on this transfer rate since the observation of separate resonances requires that the exchange rate constant for hydrogen between the two types of copper particle must be less than $\pi/\sqrt{2}$ the frequency separation of the resonances. This is ca. 1 kHz and thus the exchange rate constant must be less than 2500 s^{-1}. The relaxation time measurements in fact suggest that exchange is even slower than this, since no evidence is found for exchange of hydrogen with the support or gas phase on a timescale of tens of milliseconds.

ACKNOWLEDGMENTS

The authors thank the Catalysis Initiative of the SERC for financial support, Professor G. Webb and Dr. T. Baird for the TEM images, and a referee for suggesting the identity of the downfield site in U6649 with that of U6776.

REFERENCES

1. Dennison, P. R., Packer, K. J., and Spencer, M. S., *J. Chem. Soc., Faraday Trans. I* **85**, 3537 (1989).
2. Bendada, A., Chinchen, G. C., Clayden, N., Heaton, B. T., Iggo, J. A., and Smith, C. S., *Catal. Today* **9**, 129 (1991).
3. Wu, X., Gerstein, B. C., and King, T. S., *J. Catal.* **121**, 271 (1990).
4. Brown, D. T., Eguchi, T., Heaton, B. T., Iggo, J. A., and Whyman, R., *J. Chem. Soc., Dalton Trans.* 677(1991) and references cited therein.
5. Iggo, J. A., and Bennett, A., unpublished results.
6. Shimomura, K., Ogawa, K., Oba, M., and Kotera, Y., *J. Catal.* **52**, 191 (1978).
7. Okamoto, Y., Fukino, K., Imanaka, T., and Terranishi, S., *J. Phys. Chem.* **87**, 3740 (1983).
8. Brown Bourzutscky, J. A., Homs, N., and Bell, A. T., *J. Catal.* **124**, 73 (1990).
9. Bulko, J. B., Herman, R. G., Klier, K., and Simmons, G. W., *J. Chem. Phys.* **83**, 3118 (1979).
10. Frost, J., *Nature* **334**, 577 (1988).
11. Tohji, K., Udagawa, Y., Mizushima, T., and Ueno, A., *J. Phys. Chem.* **89**, 5671 (1985).
12. Bennett, A., Chinchen, G., Cobb, J. B., Heaton, B. T., and Iggo, J. A., in preparation.